Submitted to ADVANCED MATERIALS

DOI: 10.1002/ adma.201604424
Article type: Communication

Exciton Diffusion Length and Charge Extraction Yield in Organic Bilayer Solar Cells

Bernhard Siegmund*, Muhammad T. Sajjad, Johannes Widmer, Debdutta Ray, Christian Koerner, Moritz Riede, Karl Leo, Ifor D. W. Samuel*, Koen Vandewal*

B. Siegmund, Dr. J. Widmer, Dr. C. Körner, Prof. K. Leo, Prof. K. Vandewal
Dresden Integrated Center for Applied Physics and Photonic Materials (IAPP) and Institute for Applied Physics, Technische Universität Dresden, George-Bähr-Straße 1, 01062 Dresden, Germany
E-mail: bernhard.siegmund@iapp.de, koen.vandewal@iapp.de

Dr. M. T. Sajjad, Prof. I. D. W. Samuel
Organic Semiconductor Centre, SUPA, School of Physics & Astronomy, North Haugh, St Andrews, KY16 9SS, United Kingdom
E-mail: idws@st-andrews.ac.uk

Prof. D. Ray
Currently: Department of Electrical Engineering, I.I.T. Madras, Chennai 600036, India

Prof. M. Riede
Currently: Clarendon Laboratory, Parks Road, Oxford OX1 3PU, United Kingdom

Keywords: exciton diffusion length, charge carrier extraction, organic photovoltaics, bilayer, photocurrent modelling

Organic light emitting diodes (OLED), solar cells, and photo-detectors have proven their potential to outperform their inorganic counterparts regarding flexibility, light-weight, transparency, scalability, and fabrication costs as demonstrated by the successful comercialisation of OLEDs. Hereby, all organic opto-electronic devices share a series of electrical and optical processes mediated by a Coulombically bound electron-hole pair called an exciton. Driven by concentration gradients, these electrically neutral quasi-particles cover an average distance ℓ_d within their lifetime of typically a few nanoseconds by means of Förster or Dexter energy transfer. The so defined exciton diffusion length is one of the critical material parameters determining the performance of organic opto-electronics. Organic photovoltaics and photodetectors with a *blended* photoactive layer[1] benefit from a long ℓ_d: As the absorber phase separation can be increased, charge recombination is reduced, resulting in an increased operating voltage.[2] Meanwhile, photo-sensitive devices with a *planar* photoactive structure such as multilayer cascades[3] benefit from a long ℓ_d resulting in enhanced short-circuit currents as excitons generated further away from the charge dissociating heterojunction are harvested. For OLEDs on the other hand, a short ℓ_d for singlet excitons is required when containing both (efficient) phosphorescent and (stable) fluorescent emitter layers to confine singlet excitons to the latter.[4]

In amorphous or polycrystalline organic semiconductors, the diffusion length of singlet excitons is often 10nm or less as a result of exciton trapping.[5,6] However, reliability and comparability of ℓ_d measurements still remain an issue, even within one technique.[7-9] For example, for the thermally stable and chemically inert small molecule zinc phthalocyanine (ZnPc), reported ℓ_d-values range over one order of magnitude (see Table S1 in the Supplementary Information (SI)). Many of these differences can be attributed to a discrepancy upon modelling of the photo-current, as discussed further in Section SI.1. Therefore, this article provides a refined technique based on modelling photocurrent spectra of solar cells

comprising the material of interest. Our method gives consistent results even for rigorously differing samples architectures and the obtained diffusion length agrees well with complementary measurements based on photoluminescence (PL) quenching.

In contrast to PL based techniques, electrical measurements also allow to study ℓ_d of non-fluorescent materials. A key advantage of our photovoltaic approach is the simultaneous quantitative access to both the exciton diffusion length and the yield of charge extraction. To account for potential losses during the splitting of excitons at the donor-acceptor (DA) interface or the subsequent charge transit to the desired electrode, via recombination processes, we introduce a charge collection yield η_c. It mediates between exciton diffusion towards the DA-interface, leading to a generation flux of CT states $\varphi_{CT}(\ell_d)$, and the extracted photo-current density j_{photo} via

$$j_{photo} = e\,\eta_c\varphi_{CT}(\ell_d) \qquad (1)$$

with *e* as elementary charge.[10] The value of η_c is often hard to determine, both in experiment and simulation (details in SI.2). This uncertainty affects the accuracy of ℓ_d when determining it using **Equation 1**. On the other hand, for known exciton dynamics, steady-state or transient[11] measurements of j_{photo} seem a suitable choice to access η_c. In this study, however, we demonstrate access to ℓ_d *and* η_c at the same time, based on easy and standardised methods, namely measurements of photovoltaic external quantum efficiencies (EQE) and thin-film optics. For this purpose, we utilise a simultaneous variation of the layer thickness x_o and the excitation wavelength λ in conjunction with optical simulations.

In our exemplary study of ZnPc, we build pin-type bilayer solar cells with C_{60} as efficient quencher for ZnPc excitons.[12] This allows characterising the material in an application oriented layer sequence, as often used in organic solar cells (alternative exciton quenchers for

high band-gap absorbers are discussed in SI.3a). A first set of solar cells comprises as electron transport layer (ETL) C_{60} n-doped with $W_2(hpp)_4$ (chemical nomenclatures in Experimental Section) and as hole transport layer (HTL) BF-DPB p-doped with $C_{60}F_{36}$. As shown in **Figure 1** (top), we center the maximum of the optical field in the ZnPc layer for 680nm, a wavelength close to which ZnPc has its peak absorption (details in SI.3b). For centering, we adjust the thickness of HTL and ETL for all ZnPc thicknesses x_o by means of numerical transfer-matrix-simulations[13].

As shown in **Figure 2**, the measured EQE maximises for a ZnPc thickness x_p between 15nm and 18nm, increasing with λ. This already indicates ℓ_d to be much smaller than the absorption length which for ZnPc is above 100nm. For modelling the measured photocurrent data as function of x_o and λ, we consider the general exciton diffusion equation

$$\frac{\partial n}{\partial t} = D\frac{\partial^2 n}{\partial x^2} + G(x,t) - k_{PL}(t)\cdot n - k_{FRET}(x)\cdot n - \alpha\cdot n^2 \qquad (2)$$

where n denotes the density distribution of singlet excitons at position x in the absorber film (here ZnPc), D the diffusion coefficient and $G(x,t)$ the time dependent exciton generation profile. The radiative decay rate in absence of quencher sites is k_{PL}, whereas k_{FRET} denotes the rate of Förster resonance energy transfer (FRET) in presence of a neighbouring material with equal or smaller optical gap. α quantifies the rate for exciton-exciton-annihilation.

Exciting the samples under steady-state conditions and low intensities (translating to exciton densities far below the annihilation threshold[14] of $10^{18}cm^{-3}$) permits to apply **Equation 2** with the following simplifications: $\partial n/\partial t=0$, $k_{PL}= \tau_o^{-1}=D/\ell_d^2$, $\alpha=0$ with τ_o as intrinsic exciton lifetime. Considering only low energy photons ($\lambda>635nm$, see SI.3b) allows to draw exclusive conclusions about the exciton dynamics in ZnPc, due to its smaller optical bandgap (1.5eV) in

comparison to C_{60} (1.8eV). Furthermore, embedding ZnPc into media *m* of a greater optical gap, *p*-BF-DPB with 3.0eV and C_{60}, allows neglecting FRET dynamics and thus circumvents additional PL-studies to determine the Förster radius[15]: $k_{FRET}^{ZnPc,m} \approx 0$. Moreover, within the framework of interference based thin-film-optics[13], we find the spatial distribution of the optical field, and thus the exciton generation, to be approximately parabolic $G_\lambda(x) \approx a_\lambda x^2 + b_\lambda x + c_\lambda$ within *a single* layer (details in SI.4). As boundary conditions for our simplified diffusion equation

$$a_\lambda x^2 + b_\lambda x + c_\lambda = D\left(\frac{1}{\ell_d^2} - \frac{\partial^2}{\partial x^2}\right)n \tag{3}$$

we choose ZnPc excitons reaching the HTL to be reflected ($\partial n/\partial x$(x=ZnPc|HTL)=0, details in SI.5) and those reaching C_{60} to decay immediately into charge transfer (CT) states[16] ($n(x=\text{ZnPc}|C_{60})=0$)[12].

We obtain an analytical expression for the photo-current as a function of ℓ_d and η_c, derived as **Equation S11** in SI.6. We apply it to *simultaneously* fit all EQE spectra (solid lines) under variation of λ *and* x_o, as representatively depicted in Figure 2 for four wavelengths of the analysed interval between 635nm and 800nm (exclusive ZnPc absorption). For this purpose, η_c is assumed to be independent of λ, as wavelength independent internal quantum efficiencies have been experimentally demonstrated for both polymer and small molecule systems.[2,17] We exclude thin ZnPc layers up to a threshold thickness of x_t = 11nm from the fitting routine due to layer roughness[18] and DA inter-diffusion[8,19] (details in SI.6b). For thicker absorber layers, we model the charge extraction to be spatially uniform, as no significant concentration of recombination centers is present in the bulk of the neat absorber.[20–22]

Following this procedure unfolds an exciton diffusion length in ZnPc of ℓ_d=(10.0±0.8)nm and a collection yield of η_c =(58±6)%. Note that a successful EQE fit features a peak position x_p coinciding with the experimental data (Figure 2). As the optical field is constructed to be approximately constant in ZnPc, x_p is found in proximity to the diffusion length. However, for smaller ℓ_d it would be desirable to achieve a peak position x_p much greater than the diffusion length to still overcome the thickness threshold for uniform charge extraction ($x_p > x_t$).

For this purpose, we introduce a pronounced slope in the optical field in the absorber rising with distance to the quenching interface. It aims to extend the exciton diffusion towards this interface, at the cost of overall exciton density. A second set of solar cells (Figure 1 bottom) is prepared showing such a field gradient in absence of thicknesses variations of both transport layers. It also differs with respect to its electronic polarity through inverse layer stacking and its transport layers. Here, BPhen is used as ETL and as HTL MeO-TPD (optical gap of 2.9eV) p-doped with F_6-TCNNQ. Comparing to set 1, we observe a pronounced shift of the EQE peak position to $x_p \gtrsim 25$nm (see Figure S3 in SI.7). Taking the respective field distribution into account and assuming complete exciton reflection at the interface between ZnPc and intrinsic MeO-TPD, we obtain ℓ_d=(10.2±0.8)nm in ZnPc and a collection yield of η_c=(58±6)% which confirms the previous results within the measurement uncertainty.

The agreement of the fitted values proves the modelling approach to be independent of the considered device geometry and underlines the thickness of maximum photo-current x_p typically not be identical with ℓ_d. Furthermore, the result implies equally efficient charge extraction for the transport layers of set 1 and 2, as expected. For both device architectures, CT-states at the DA-interface formed upon successful exciton diffusion are inefficiently harvested as extracted photo-current. This can be attributed to incomplete CT dissociation and has been observed in ZnPc-C_{60}-cells before by Rand *et al.*[23] The authors attributed this

finding to an unfavourable orientation of the ZnPc molecules with regard to the interface with C_{60}. Beyond, the measurements recorded in such an exciton diffusion study can be used to evaluate the potential of a corresponding blended absorber system as discussed in SI.8.

To obtain an independent confirmation of the outlined method, an alternative method to determine ℓ_d based on the transient decay of PL is performed.[8,24] A sequence of ZnPc thin-films with varying layer thickness is prepared on quartz glass substrates in the absence and presence of 50nm C_{60}, as shown in **Figure 3** (top). The ZnPc-C_{60}-interface acts as a complete quencher[12] and reduces the effective exciton lifetime. Meanwhile, ZnPc excitons at the interface with quartz glass or vacuum are expected to reflect, with vacuum being known as an imperfectly reflecting medium.[25] For a conjoint analysis (details in SI.9) of both thin-film sets, a remarkably good agreement is obtained between all measured and modelled PL decays (Figure 3 bottom). The diffusion length ℓ_d= (9.6±0.8)nm is obtained using a Förster radius of (1.4±0.4)nm, and agrees well with the value obtained via spectral modelling, presented earlier. As the interface between ZnPc and vacuum is modelled to completely reflect excitons, it yields the possibility of a slight underestimation of ℓ_d.

In summary, we have demonstrated an experimentally easily accessible approach to determine the singlet exciton diffusion length ℓ_d. We demonstrate its validity using ZnPc as an example but believe it to be applicable to a wider range of organic absorbers. The analysis involves i) preparing a series of bilayer solar cells with varying absorber thickness, ii) measuring their external quantum efficiency spectra, and iii) evaluating the respective device optics. The approach allows the determination of the exciton diffusion length and also the product of the combined yield of charge-transfer state dissociation with subsequent charge extraction η_c. For ZnPc-C_{60} as photoactive system, this procedure yields an exciton diffusion length in ZnPc ℓ_d of (10.1±0.9)nm and η_c = (58±6)%. Two rigorously differing solar cell architectures were

studied and give consistent results. The value of ℓ_d is furthermore in excellent agreement with time resolved measurements of photoluminescence quenching resulting in a diffusion length ℓ_d of (9.6±0.8)nm, which underlines the reliability of the newly proposed method.

Experimental Section

Preparation of solar cells: Substrates with pre-structured indium tin oxide (ITO, 90nm, 32Ω/□, Thin Films Devices, USA) are purchased as bottom electrode. All organic and metal layers are deposited via thermal evaporation in ultra high vacuum (K. J. Lesker, UK) with a base pressure of around 10^{-8} mbar. Quartz crystal micro-balances are used to monitor the deposition rates (for organics 0.3-0.4 Å/s) and thus to control layer thicknesses and doping ratios. Set 1 follows *nip*-type layer sequence (40nm-x_o/2) of C_{60} n-doped with 3 weight(wt)% Tetrakis(1,3,4,6,7,8-hexahydro-2H-pyrimido[1,2-a]pyrimidinato)ditungsten(II) ($W_2(hpp)_4$), 20nm of intrinsic C_{60}, x_o of ZnPc (Supplier: TCI Europe N.V., Belgium), (82nm-x_o/2) of N4,N4'-bis(9,9-dimethyl-9H-fluoren-2-yl)-N4,N4'-diphenylbiphenyl-4,4'-diamine (BF-DPB) p-doped with 10 wt% $C_{60}F_{36}$, and 100nm of aluminium (Al) as reflecting top electrode (photoactive area of 6.4mm^2). Set 2 follows the *pin*-type sequence 1nm of dopant 2,2'-(perfluoronaphthalene-2,6-diylidene)dimalononitrile (F_6-TCNNQ), 20nm of N,N,N',N'-tetrakis(4-methoxyphenyl)-benzidine (MeO-TPD) p-doped with 2wt% F_6-TCNNQ, 5nm of intrinsic MeO-TPD, x_o of ZnPc, 20nm of C_{60}, 6nm of 4,7-diphenyl-1,10-phenanthroline (BPhen) and 100nm of Al. Besides the n-dopant $W_2(hpp)_4$, all organic materials are purified at least once by vacuum gradient sublimation. After deposition, both sets are sealed under nitrogen with a cover glass and a humidity getter via a UV-hardened epoxy glue.

Analysis of solar cells: For measuring the EQE, xenon light (Oriel Xe Arc-Lamp Apex Illuminator, Newport, US) is filtered to 5nm spectral width with a monochromator (Cornerstone 260 1/4 m Monochromator, Newport, US). Excitation light chopped at 215Hz excites the sample on a mask area of 2.8 mm^2. j_{photo} is detected via a lock-in amplifier (Signal

Recovery SR 7265, National Instruments, US). A calibrated silicon diode (S1337, Hamamatsu, Japan) monitors the excitation intensity. A compact CCD spectrometer (USB4000, Ocean Optics, US) reads out the relative excitation spectrum. The optical constants are determined via transmission and reflection (UV-3100 Spectrometer, Shimadzu, Japan) of thin films with varying layer thickness and subsequent optical modelling.

Preparation of PL quenching samples: The same evaporation system is used to deposit thin films of ZnPc and optionally C_{60} onto quartz substrates. Storing and analysis of the sample are performed under vacuum.

Analysis of PL quenching samples: Samples are excited with 100fs pulses at 400nm from a frequency doubled Ti:Sapphire laser. The subsequent decay of the PL is detected between 810nm and 830nm with a time resolution of ~2ps via a streak camera (C6860, Hamamatsu, Japan) in synchroscan mode with the laser at 80MHz.

Supporting Information
Supporting Information is available from the Wiley Online Library or from the author.

Acknowledgements
We thank the German BMBF for funding within the scope of the projects InnoProfile 2.2 (03IPT602X) and MEDOS (03EK3503A) as well as the European Commission within the scope of Career Integration Grant (FP7, MSCA, 630864). We also thank Caroline Walde and Andreas Wendel from IAPP for sample preparation as well as Dr. Mauro Furno and Sim4tec for providing the software for optical transfer matrix calculations. I.D.W.S. and M.T.S. acknowledge support from the European Research Council (grant number 321305) and from EPSRC (grant number EP/L017008/1). I.D.W.S. also acknowledges a Royal Society Wolfson Research Merit Award. K.L. is a fellow of the Canadian Institute for Advanced Research (CIFAR).

Received: ...
Revised: ...
Published online: ...

[1] R. Meerheim, C. Körner, B. Oesen, K. Leo, *Appl. Phys. Lett.* **2016**, *108*, 103302.

[2] K. Vandewal, S. Albrecht, E. T. Hoke, K. R. Graham, J. Widmer, J. D. Douglas, M. Schubert, W. R. Mateker, J. T. Bloking, G. F. Burkhard, A. Sellinger, J. M. J. Fréchet, A. Amassian, M. K. Riede, M. D. McGehee, D. Neher, A. Salleo, *Nat. Mater.* **2014**, *13*, 63.

[3] K. Cnops, B. P. Rand, D. Cheyns, B. Verreet, M. A. Empl, P. Heremans, *Nat. Commun.* **2014**, *5*, 3406.

[4] Y. Sun, N. C. Giebink, H. Kanno, B. Ma, M. E. Thompson, S. R. Forrest, *Nature* **2006**, *440*, 908.

[5] S. Athanasopoulos, E. Hennebicq, D. Beljonne, A. B. Walker, *J. Phys. Chem. C* **2008**, *112*, 11532.

[6] O. V. Mikhnenko, M. Kuik, J. Lin, N. Van Der Kaap, T.-Q. Q. Nguyen, P. W. M. Blom, *Adv. Mater.* **2014**, *26*, 1912.

[7] J. D. A. Lin, O. V. Mikhnenko, J. Chen, Z. Masri, A. Ruseckas, A. Mikhailovsky, R. P. Raab, J. Liu, P. W. M. Blom, M. A. Loi, C. J. García-Cervera, I. D. W. Samuel, T.-Q. Nguyen, *Mater. Horizons* **2014**, *1*, 280.

[8] P. E. Shaw, A. Ruseckas, I. D. W. Samuel, *Adv. Mater.* **2008**, *20*, 3516.

[9] M. T. Sajjad, A. J. Ward, C. Kästner, A. Ruseckas, H. Hoppe, I. D. W. Samuel, *J. Phys. Chem. Lett.* **2015**, *6*, 3054.

[10] A. K. Ghosh, T. Feng, *J. Appl. Phys.* **1978**, *49*, 5982.

[11] T. K. Mullenbach, R. J. Holmes, *Appl. Phys. Lett.* **2015**, *107*, 123303.

[12] Y. Terao, H. Sasabe, C. Adachi, *Appl. Phys. Lett.* **2007**, *90*, 103515.

[13] L. A. A. Pettersson, L. S. Roman, O. Inganäs, *J. Appl. Phys.* **1999**, *86*, 487.

[14] A. J. Lewis, A. Ruseckas, O. P. M. Gaudin, G. R. Webster, P. L. Burn, I. D. W. Samuel, *Org. Electron.* **2006**, *7*, 452.

[15] W. A. Luhman, R. J. Holmes, *Adv. Funct. Mater.* **2011**, *21*, 764.

[16] K. Vandewal, K. Tvingstedt, A. Gadisa, O. Inganäs, J. V. Manca, *Phys. Rev. B* **2010**, *81*, 125204.

[17] K. Vandewal, Z. F. Ma, J. Bergqvist, Z. Tang, E. G. Wang, P. Henriksson, K. Tvingstedt, M. R. Andersson, F. L. Zhang, O. Inganas, *Adv. Funct. Mater.* **2012**, *22*, 3480.

[18] C. Schünemann, C. Elschner, A. A. Levin, M. Levichkova, K. Leo, M. Riede, *Thin Solid Films* **2011**, *519*, 3939.

[19] M. Drees, R. M. Davis, J. R. Heflin, *Phys. Rev. B* **2004**, *69*, 165320.

[20] F. Yang, S. R. Forrest, *ACS Nano* **2008**, *2*, 1022.

[21] A. Foertig, A. Wagenpfahl, T. Gerbich, D. Cheyns, V. Dyakonov, C. Deibel, *Adv. Energy Mater.* **2012**, 1483.

[22] W. Tress, A. Petrich, M. Hummert, M. Hein, K. Leo, M. Riede, *Appl. Phys. Lett.* **2011**, *98*, 063301.

[23] B. P. Rand, D. Cheyns, K. Vasseur, N. C. Giebink, S. Mothy, Y. Yi, V. Coropceanu, D. Beljonne, J. Cornil, J. L. Brédas, J. Genoe, *Adv. Funct. Mater.* **2012**, *22*, 2987.

[24] A. J. Ward, A. Ruseckas, I. D. W. Samuel, *J. Phys. Chem. C* **2012**, *116*, 23931.

[25] O. V Mikhnenko, F. Cordella, A. B. Sieval, J. C. Hummelen, P. W. M. Blom, M. A. Loi, *J. Phys. Chem. B* **2009**, 9104.

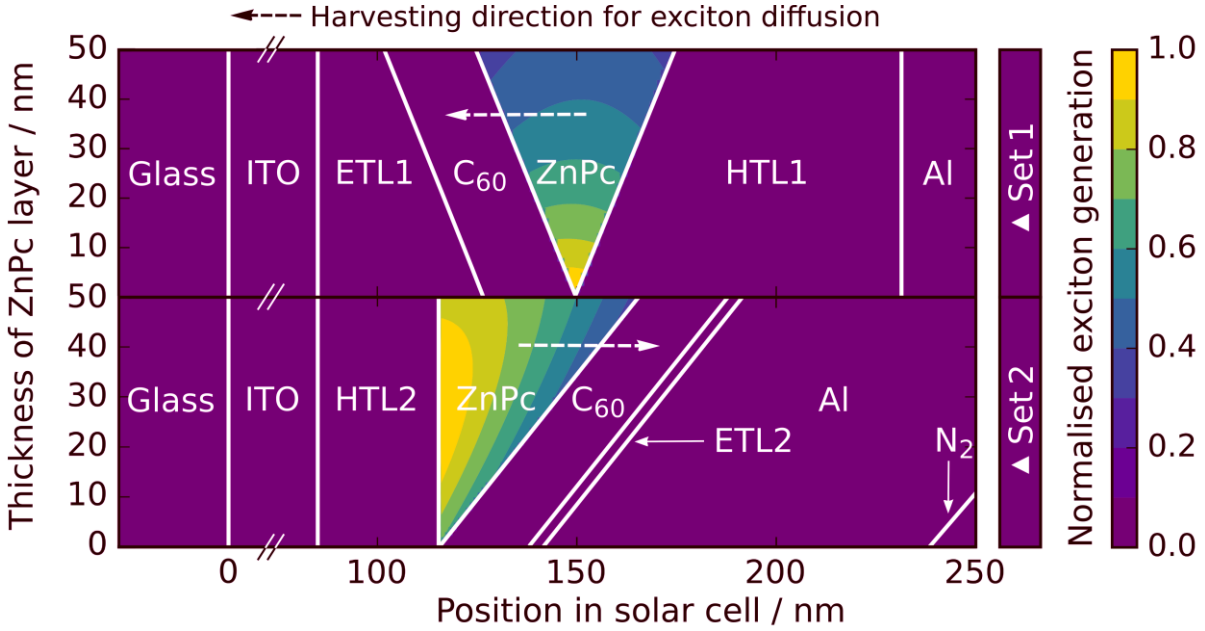

Figure 1. Composition and simulation of the exciton generation profile of the solar cell sets 1 and 2 under variation of the ZnPc layer thickness x_o when excited with a wavelength of 680nm. The device sets differ in their i) electronic polarity, ii) choice of transport layers (ETL1=n-doped C_{60}, ETL2=intrinsic BPhen, HTL1=p-doped BF-DPB, HTL2=intrinsic MeO-TPD (5nm, touching ZnPc) followed by p-doped MeO-TPD) and iii) optical field distribution in ZnPc: Each device of set 1 exhibits an approximately homogeneous field, as illustrated for example for the device x_o=24nm whose field fluctuations are restricted to only 5%. The optical profiles for solar cells of set 2, in contrast, describe a distinct slope in the ZnPc layer whose amplitude decreases towards the quenching C_{60} interface, for instance for x_o=24nm by about 50%.

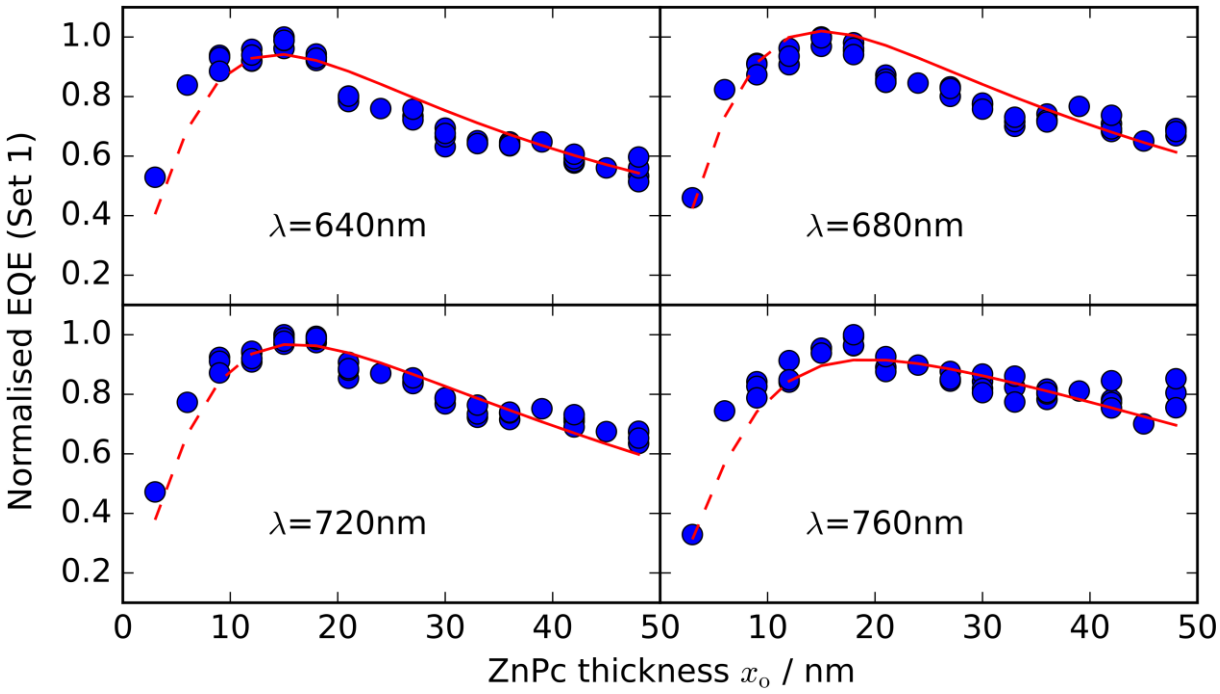

Figure 2. External quantum efficiency (EQE) of set 1 from Figure 1 under variation of the layer thickness of ZnPc x_o and the excitation wavelength λ. The experimental data (circles) is jointly fitted (solid lines) for all x_o and λ according to Equation S11 in SI.6. The dashed lines indicate the prolongation of the fit for the range of discarded samples ($x_o \leq 11$nm). The extracted diffusion length in ZnPc is ℓ_d=(10.0±0.8)nm and the charge extraction yield is η_c= (58±6)%. For better readability, the EQE is normalised to its experimental maximum for each sub-graph, namely to 18.1%, 15.3%, 13.4% and 7.5% (read for increasing wavelength).

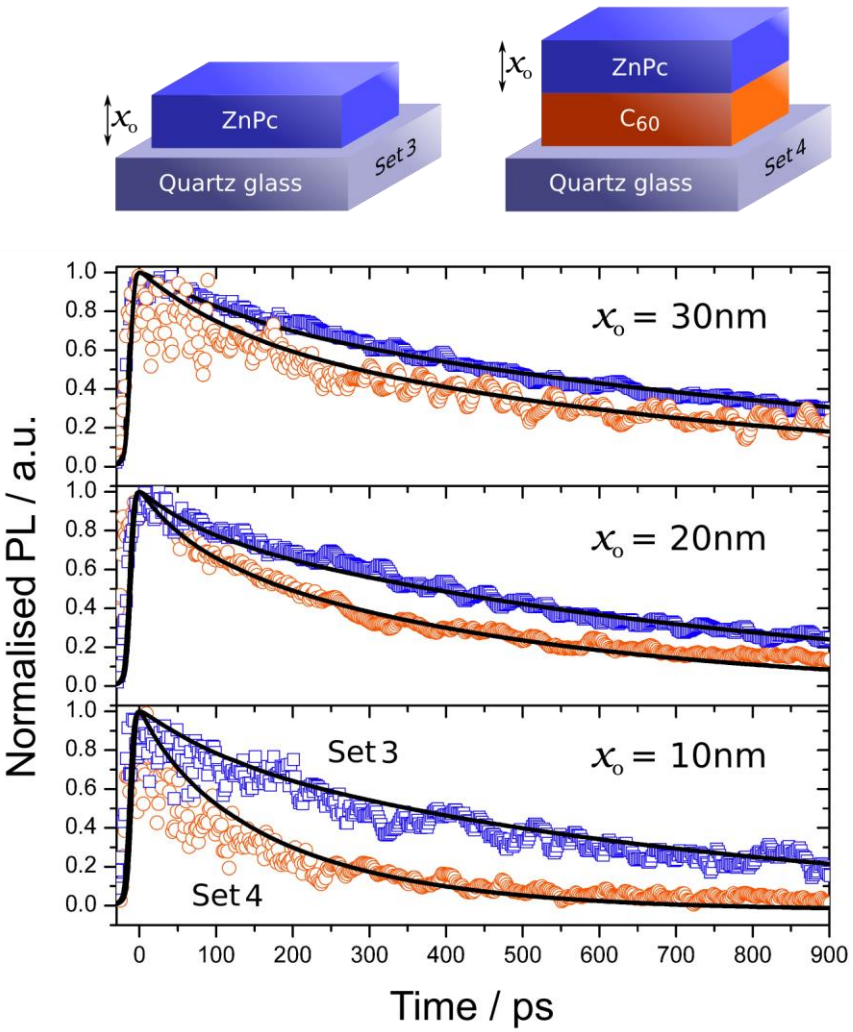

Figure 3. Top: Schematics of the series of investigated thin films with a thickness variation of ZnPc. **Bottom:** Corresponding experimental time-resolved fluorescence decays measured using a detection wavelength range of 810-830nm. The wavelength of 400nm is used to excite the samples. The bare absorber on quartz glass (set 3, top signal as blue squares) is analysed in conjunction with the corresponding sample with a quenching C_{60} sublayer (set 4, bottom signal as orange circles). The best fit (black line) using Equation 2 (G=0, α=0) is obtained for ℓ_d=(9.6±0.8)nm and a Förster radius of (1.4±0.4)nm.

ToC entry:

A method for resolving the diffusion length of excitons and the extraction yield of charge carriers is presented based on the performance of organic bilayer solar cells and careful modeling. The technique uses a simultaneous variation of the absorber thickness and the excitation wavelength. Rigorously differing solar cell structures as well as independent photoluminescence quenching measurements give consistent results.

Keyword:
exciton diffusion length, charge carrier extraction, organic photovoltaics, bilayer, photocurrent modelling

B. Siegmund*, M. T. Sajjad, J. Widmer, D. Ray, C. Koerner, M. Riede, K. Leo, I. D. W. Samuel*, K. Vandewal*

Title:
Exciton Diffusion and Charge Carrier Extraction in Organic Bilayer Solar Cells

ToC figure